Journal Pre-proofs

Soluplus® promotes efficient transport of meloxicam to the central nervous system via nasal administration

Bence Sipos, Zsolt Bella, Ilona Gróf, Szilvia Veszelka, Mária A. Deli, Kálmán F. Szűcs, Anita Sztojkov-Ivanov, Eszter Ducza, Róbert Gáspár, Gábor Kecskeméti, Tamás Janáky, Balázs Volk, Mária Budai-Szűcs, Rita Ambrus, Piroska Szabó-Révész, Ildikó Csóka, Gábor Katona

PII: S0378-5173(23)00014-5
DOI: https://doi.org/10.1016/j.ijpharm.2023.122594
Reference: IJP 122594

To appear in: *International Journal of Pharmaceutics*

Received Date: 20 October 2022
Revised Date: 15 December 2022
Accepted Date: 5 January 2023

Please cite this article as: B. Sipos, Z. Bella, I. Gróf, S. Veszelka, M.A. Deli, K.F. Szűcs, A. Sztojkov-Ivanov, E. Ducza, R. Gáspár, G. Kecskeméti, T. Janáky, B. Volk, M. Budai-Szűcs, R. Ambrus, P. Szabó-Révész, I. Csóka, G. Katona, Soluplus® promotes efficient transport of meloxicam to the central nervous system via nasal administration, *International Journal of Pharmaceutics* (2023), doi: https://doi.org/10.1016/j.ijpharm.2023.122594

Soluplus® promotes efficient transport of meloxicam to the central nervous system via nasal administration

Bence Sipos[a], Zsolt Bella[b], Ilona Gróf[c], Szilvia Veszelka[c], Mária A. Deli[c], Kálmán F. Szűcs[d], Anita Sztojkov-Ivanov[e], Eszter Ducza[e], Róbert Gáspár[d], Gábor Kecskeméti[f], Tamás Janáky[f], Balázs Volk[g], Mária Budai-Szűcs[a], Rita Ambrus[a], Piroska Szabó-Révész[a], Ildikó Csóka[a], Gábor Katona[a, *]

[a] Institute of Pharmaceutical Technology and Regulatory Affairs, Faculty of Pharmacy, University of Szeged, Eötvös Str. 6, H-6720 Szeged, Hungary

[b] Department of Oto-Rhino-Laryngology and Head-Neck Surgery, University of Szeged, Tisza Lajos Blvd. 111, H-6725 Szeged, Hungary

[c] Institute of Biophysics, Biological Research Centre, Szeged, Temesvári Blvd. 62, H-6726 Szeged, Hungary

[d] Department of Pharmacology and Pharmacotherapy, Albert Szent-Györgyi Medical School, Faculty of Medicine, University of Szeged, Hungary

[e] Department of Pharmacodynamics and Biopharmacy, Faculty of Pharmacy, University of Szeged, Eötvös Str. 6, H-6720 Szeged, Hungary

[f] Department of Medical Chemistry, Interdisciplinary Excellence Centre, University of Szeged, Dóm square 8, H-6720 Szeged, Hungary

[g] Directorate of Drug Substance Development, Egis Pharmaceuticals Plc., Keresztúri Str. 30 – 38, H-1106 Budapest, Hungary

* Correspondence: Gábor Katona; katona.gabor@szte.hu

Graphical abstract

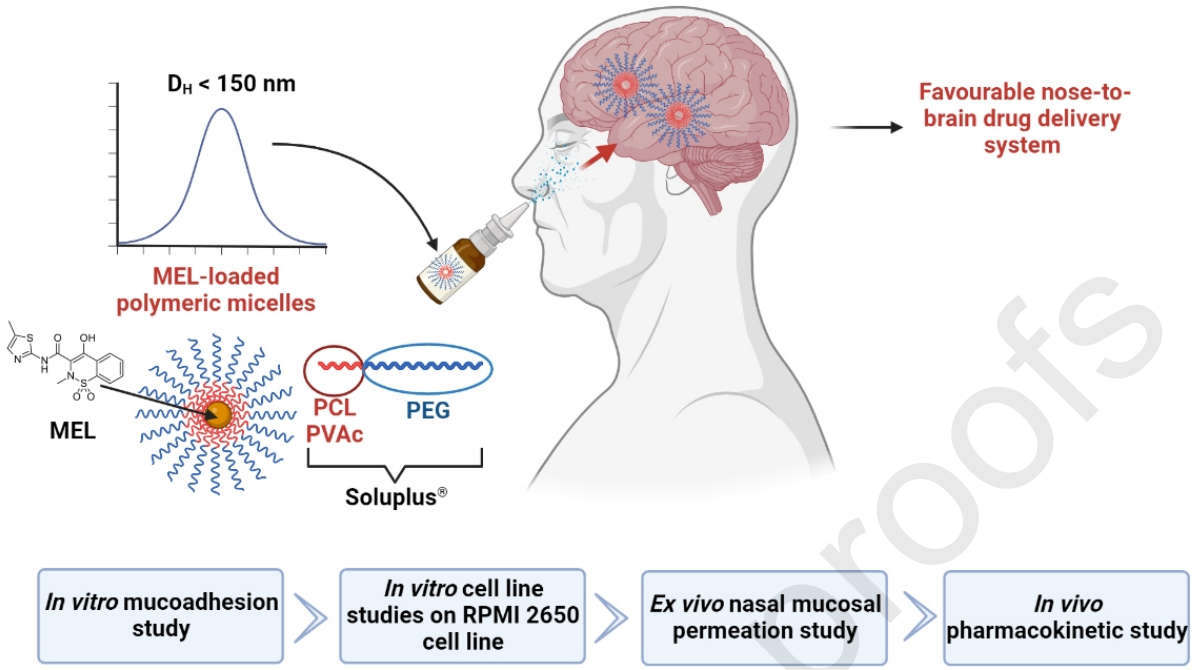

Abstract

In our present series of experiments, we investigated the nasal applicability of the previously developed Soluplus® - Meloxicam polymeric micelle formulation. Utilizing the nasal drug investigations, moderately high mucoadhesion was experienced in nasal conditions which alongside the appropriate physicochemical properties in liquid state, contributed to rapid drug absorption through human RPMI 2650 cell line. *Ex vivo* studies also confirmed that higher nasal mucosal permeation could be expected with the polymeric micelle nanoformulation compared to a regular MEL suspension. Also, the nanoformulation met the requirements to provide rapid drug permeation in less 1 hour of our measurement. The non-toxic, non-cell barrier damaging formulation also proved to provide a successful passive transport across excides human nasal mucosa. Based on our *in vivo* investigations, it can be concluded that the polymeric micelle formulation provides higher meloxicam transport to the central nervous system followed by a slow and long-lasting elimination process compared to prior results where physical particle size reduction methods were applied. With these results, a promising solution and nanocarrier is proposed for the successful transport of non-steroidal anti-inflammatory drugs with acidic character to the brain.

Keywords

Nasal administration; Polymeric micelle; Meloxicam; Permeability enhancement; Brain

1. Introduction

Administration of drugs to the central nervous system (CNS) is a challenging area in the medical field due to its many biological and pharmaceutical technological aspects. The need for efficient treatment of various CNS-related diseases is of paramount importance in today's research and development processes. The increasing prevalence of neurodegenerative diseases (such as Alzheimer's Disease, Parkinson's Disease etc.) holds the demand for novel and innovative products on the market which may help in their efficient therapy (Goldsmith et al., 2014; Saraiva et al., 2016). The problem also lies in the fact that potential drug candidates of these diseases cannot access the CNS in a sufficient concentration for clinical investigations. This challenge requires novel drug delivery systems, which are suitable for efficient transport to the CNS, where a drug concentration sufficient for further investigations would be achieved (Wohlfart et al., 2012; Wong et al., 2019).

These neurodegenerative diseases are often associated with the inflammation of brain tissue, the so-called neuroinflammation (Sharma 2011; Shabab et al., 2016). The mechanism behind this condition is that the inflammatory cytokine balance is disrupted towards the emergence of the pro-inflammatory cytokines such as cyclooxygenase (COX). The treatment of COX enzyme-mediated neuroinflammation plays a pivotal role and holds a high demand in the field of unmet clinical needs (Choi et al., 2013; Heneka et al., 2015). Current potential drug candidates are hindered by their inability to bypass the blood-brain barrier (BBB) (Szabó-Révész, 2018). Epidemiological studies proved that long-term use of non-steroidal anti-inflammatory agents (NSAIDs) decrease the risk of Alzheimer's Disease and prolongs its prognosis (McGeer and McGeer, 2007; Pasqualetti et al., 2009). *In vitro* and *in vivo* studies also proved that COX inhibition helps with the symptoms of neuroinflammation. Therefore, the possibility of introducing NSAIDs as COX enzyme inhibitors to the CNS represents a promising solution. The main protection mechanism is based on mitochondria depolarization and the inhibition of calcium uptake. This is possible due to the ionizable carboxylic groups of the NSAIDs, which have a similar effect to mild mitochondrial uncouplers (Calvo-Rodríguez et al., 2015; Sanz-Blasco et al., 2018).

Polymeric micelles are one of the novel nanocarriers. These nanomedicines can offer increased solubility, enhanced drug release and permeability through biological barriers. Polymeric micelles are made up by the so-called amphiphilic graft co-polymers, which just like classic micellar systems prepared by surfactants, tend to self-associate above the critical micellar concentration (CMC) and temperature, allowing a highly efficient drug encapsulation (Sipos et al., 2020; Ghezzi et al., 2021; Sipos et al., 2022). Generally, they can be described as non-toxic agents and they do not harm the cell membranes, less likely than in case of classic surfactant-like molecules (Zakharova et al., 2019; Katona et al., 2022). Their main advantage might lie in the fact that they can transport poorly water soluble active pharmaceutical ingredients (APIs) with low permeation tendency across biological barriers difficult to get through, such as the BBB (Sun et al., 2020). Based on the molecular weight of the co-polymer, the surface charge, the presence of surface modifying ligands and the desired route, various transport mechanisms can be experienced. Polymeric micelles with positively charged surface usually accumulate in the mucus layer followed by the passive diffusion of the drug. This mechanism is usually

exploited when a local effect is desired with rapid onset of action. Polymeric micelles with negative charge or without charge on the micellar surface can be categorized as mucopenetrating micelles, where the biological mucus layer allows the micellar carriers to be absorbed via transcytosis or paracellular transport (Pepic et al., 2013). With proper characterization of the micellar system via the determination of zeta potential, as the value of the surface charge in liquid state, the therapeutic aspects can be taken into consideration prior to administration or even prior to drug selection. Moreover, micellar systems presenting polyethylene glycol (PEG) and other hydrophilic moieties at their surface are less prone to the scavenging process by the macrophages (Thotakura et al., 2020). This holds the information that PEG-based copolymers are more stable in circulation, allowing a higher residence time and protection against the biological environmental conditions, unlike co-polymers which are based for instance on polylactic acid (PLA) showing lower stability (Watanabe et al., 2006; Owen et al., 2012).

Besides choosing the proper drug and nanocarrier, the adequate administration route is just as important. By administering nanomedicines via the nasal route, a higher bioavailability can be achieved (Sabir et al., 2021). This is due to the fact that the nasal mucosa is highly vascularized with a large surface allowing a prominent drug transport across this barrier (Warnken et al., 2016; Sipos et al., 2021). After administration, the drug and the drug-loaded carrier system can take up on two pathways. The first is the nose-to-blood transport route, where the penetration occurs across the nasal mucosa followed by a rapid uptake to the blood vessels. Speaking of brain targeting, the absorbed substance can circulate through the body prior to drug and/or drug-loaded carrier absorption through the BBB (Khan et al., 2017). Polymeric micelles are among the best carrier systems for this role, as they show high circulation and dilution stability under these conditions (Owen et al., 2012). The other main advantage is the nose-to-brain pathway, which is made possible by the high innervation of olfactory nerves in the nasal mucosa (Pardeshi and Belgamwar, 2013). This allows a rapid solution to bypass the BBB where the intact carrier and/or drug can travel across the nerval pathways directly to the brain (Khan et al., 2017; Li et al., 2017). The concrete mechanism has been not yet fully explored in case of polymeric micelles; however, the beneficial effects can be experienced in case of enhanced brain targeting. Furthermore, studies have proven that Alzheimer's Disease most likely begins in the nerve network of the olfactory region where initial amyloid plaque formation can appear (Agrawal et al., 2018).

Previously, we developed a meloxicam (MEL)-loaded Soluplus® (SP) polymeric micelle system (SP-MEL) for nasal administration which has been structurally and *in vitro* tested for nasal administration (Sipos et al., 2020). SP was chosen as a biodegradable co-polymer which has a low toxicity potential ($LD_{50,\ oral}$ > 5,000 mg/kg) besides the high solubilization capacity. The encapsulation was performed by utilizing SP which has a low CMC value in water besides its non-toxic behavior. The nanoparticles had an average particle size of 100.47 nm in monodisperse distribution with a polydispersity index (PdI) of 0.149 and high colloidal stability with a zeta potential of – 26.7 mV preventing colloidal aggregation. Small and uniform particle size contributes to a uniform and rapid drug absorption profile across mucosal barriers, that is why it is important to keep the PdI as low as possible, most commonly below 0.300. The negative surface charge as explained above also contributes to carrier-intact paracellular or

transcytosis-based take-up mechanisms. The physicochemical characteristics of the dissolved product meets the requirements of the nasal administration. Its hypotonic nature (240 mOsmol/l) can increase drug absorption alongside with the permeation enhancing effect of SP (Hong et al., 2019). The viscosity of the formulation (32.5 mPas) is also suitable to form an intranasal liquid formulation as it can be administered as a nasal drop or a spray. This low viscosity also contributes to a faster drug release as highly viscous formulation result in slower diffusion from the carrier matrix. The SP-MEL formulation provided a higher drug release in simulated nasal conditions as well as high drug absorption through artificial membranes.

Our goal with this present series of experiments is to justify that SP can efficiently promote the transport of MEL, a model drug with low water solubility and brain permeability to the CNS. Our hypothesis is that via nasal administration, higher concentrations of MEL can be achieved in the CNS. By the formulation of the nanocarrier, the administration of small molecular weight NSAIDs can be achieved. This would lead to gain an adequate concentration of the API in the central nervous system and it would open up the possibility to perform a better executed clinical trials later on to further describe the beneficial effects of NSAIDs in the treatment of neuroinflammation. To confirm our previous *in vitro* results, we performed nasal applicability studies starting from mucoadhesion and cell line studies, *ex vivo* penetration studies and we investigated the *in vivo* pharmacokinetics of this formulation.

2. Materials and methods

2.1. Materials

MEL (4-hydroxy-2-methyl-N-(5-methyl-2-thiazolyl)-2H-1,2-benzothiazine-3-carboxamid-1,1-dioxide) was applied as a model drug in our studies and acquired from EGIS Pharmaceuticals Plc. (Budapest, Hungary). Soluplus® (SP, polyvinyl caprolactam – polyvinyl acetate – polyethylene glycol graft co-polymer (PCL-PVAc-PEG)) as a micelle-forming agent was kindly gifted from BASF GmbH (Hannover, Germany). Simulated Nasal Electrolyte Solution (SNES) as a simulated nasal fluid was applied during some measurements which is composed of 8.77 g sodium chloride, 2.98 g potassium chloride, 0.59 g anhydrous calcium chloride in 1000 ml of deionized water at pH 5.6 (Castile et al., 2013). Chemicals for SNES as well as disodium phosphate, monopotassium phosphate for pH 7.4 phosphate-buffered saline (PBS) solution and all the other excipients for our measurements were acquired from Sigma-Aldrich Co. Ltd. (Budapest, Hungary) unless otherwise indicated.

2.2. Formulation of MEL-loaded polymeric micelles

For each investigation, formulations were prepared freshly, utilizing the thin-film hydration formulation method, which proved to be successful previously after factorial design-based optimization (Sipos et al., 2020). Briefly, 15 mg of MEL was weighed into a beaker, it was dissolved with a few drops of 0.1 M sodium hydroxide solution (NaOH) and 10 ml of ethanol. 100 mg SP was added and the resulting solution was concentrated with a Büchi R-210 (Büchi, Flawil, Switzerland) rotary vacuum evaporator (50 °C with gradually decreasing pressure from 1000 to 100 bar with a rate of 50 bar/min, followed by 10 to 15 minutes of drying at 100 bar). After hydration of the polymeric film with purified water, the pH was adjusted between 5.6 and 7.4 and 5 % w/v D-trehalose dihydrate was dissolved with the formulation. Therafter, 1 ml

aliquots were freeze-dried at – 40 °C for 12 h under a 0.013 mbar pressure with additional 3 h secondary drying at 25 °C using a ScanVac CoolSafe 100-9 (LaboGene, ApS, Lynge, Denmark) laboratory apparatus. After the freeze-drying process, samples were redispersed in a nominal MEL concentration of 2.5 mg/ml.

2.3. Dynamic light scattering measurements (DLS)

Prior to each investigation, the freshly prepared samples were evaluated via dynamic light scattering using a Malvern Zetasizer Nano ZS (Malvern Instruments, Worcestershire, UK) apparatus. The water dispersed freeze-dried cakes were measured at 25 °C in folded capillary cells with a set refractive index of 1.72. Each measurement was carried out in triplicate. The acceptance criteria were the following: average hydrodynamic diameter between 80 to 150 nm, with a PdI less than 0.300 and a zeta potential below – 20 mV. If the formulation met these requirements, it was selected for further investigations demonstrated in this article.

2.4. Quantification of MEL concentration via HPLC

To determine the concentration of MEL during the experiments, high performance liquid chromatography (HPLC) was performed using an Agilent 1260 (Agilent Technologies, Santa Clara, CA, USA) device. The stationary phase was a Kinetex® C18 column (5 µm, 150 mm x 4.6 mm (Phenomenex, Torrance, CA, USA)). The injection volume was 10 µl. The temperature was set at 30 °C. As mobile phases, a 0.065 M KH_2PO_4 solution adjusted to pH 2.8 with phosphoric acid (A) and methanol (B) were used. A two-step gradient elution was used for the separation. The starting proportion of 50 % A eluent was reduced to 25 % in 14 minutes, and then raised again to 50 % in 20 minutes. The eluent flow rate was 1 ml/min and the detection of the chromatograms was carried out at 355 ± 4 nm using UV-Vis diode array detector. Data were evaluated using a ChemStation B.04.03 software (Agilent Technologies, Santa Clara, CA, USA). The retention time of MEL was detected at 14.34 min. The determined limit of detection (LOD) and quantification (LOQ) were 16 ppm and 49 ppm, respectively (Sipos et al., 2020).

2.5. *In vitro* mucoadhesion study

To investigate the mucoadhesive properties of the SP-MEL formulation via tensile test, a TA-XT Plus (Texture Analyser (Metron Ltd., Budapest) instrument equipped with a 5 kg load cell and a 1 cm-in-diameter cylinder probe was used (Horváth et al., 2015; Budai-Szűcs et al., 2018). The SP-MEL formulation and blank SP solution were placed in contact with a wetted filter paper. For wetting, 50 µl of an 8 % w/w mucin dispersion as simulated mucosal membrane was used, where the mucin dispersion was prepared with a pH 5.6 SNES. 5 parallel measurements were performed. 20 mg of the samples was attached to the probe and placed in contact with the mucin wetted filter paper. A 2500 mN preload was used for a duration of 3 minutes and the cylinder probe was moved upwards separating the sample from the substrate with a prefixed speed of 2.5 mm/min. The adhesive force as the maximum detachment force and the work of adhesion were measured. The work of adhesion was calculated as the area (AUC) under the force versus distance curve. The formulations were thermostated at 37 °C for 30 minutes before the measurement and the experiment was carried out at this temperature. As references, SP and the SP-MEL formulation were measured without the presence of mucin as negative controls,

and as positive controls, 0.5 % w/v hyaluronic acid solution was applied due to its well-known mucoadhesive properties.

2.6. Cell cultures

Human nasal epithelial cells (RPMI 2650; ATCC cat. no. CCL 30) were grown in Dulbecco's Modified Eagle's Medium (DMEM, Gibco, Life Technologies, USA) supplemented with 10% fetal bovine serum (FBS, Pan-Biotech GmbH, Germany) in a humidified 37 °C incubator in presence of 5% carbon dioxide and 50 µg/ml gentamicin in order to prevent infection of the cells. The surfaces of the culture dishes were coated with 0.05% rat tail collagen dissolved in sterile distilled water before cell seeding and the medium was changed every 2 days. When RPMI 2650 cells reached approximately 80 – 90% confluency in the dish, they were trypsinized with 0.05% trypsin and 0.02% EDTA solution. One day before the experiment, retinoic acid (10 µM) and hydrocortisone (500 nM) were added to the cells to form a tighter barrier (Kürti et al., 2013a). For the permeability measurements, epithelial cells were co-cultured with human vascular endothelial cells to create a more physiological barrier representing both the nasal epithelium and the submucosal vascular endothelium (Pedroso et al., 2011; Cecchelli et al., 2014). The human vascular endothelial cells were differentiated from $CD34^+$ stem cells isolated from human umbilical cord blood as described earlier (Pedroso et al., 2011). Frozen batches of human vascular endothelial cells were received from the Laboratoire de la Barrière Hémato-Encéphalique, University of Artois, Lens, France. The endothelial cells were grown in endothelial culture medium (ECM-NG, Sciencell, USA) supplemented with 5% FBS, 1% endothelial growth supplement (ECGS, Sciencell, USA) and 0.5% gentamicin on 0.2% gelatine-coated culture dishes (10 cm diameter). For the permeability experiment, cells were used at passage 8.

2.7. Cell viability assay

To follow cell damage and/or protection in living barrier forming cells and to quantify the viability of adherent cells, real-time cell electronic sensing technique was used. To register the impedance of cell layers, a RTCA-SP instrument (ACEA Biosciences, USA) was used. The registration took place every 10 min and the cell index was defined at each time point. The cell index was defined as $(R_n - R_b)/15$, where R_n is the cell-electrode impedance of the wall when it contains cells and R_b is the background impedance. E-plates with 96-well and built-in gold electrodes were coated in 0.2% gelatine and placed for 20 min in the incubator. After the incubation, the gelatine was removed and 50 µl of the culture medium was added to each well. The dispensed RPMI 2650 cell suspension had a density of 2×10^4 cells/well. When cells reached a steady growth phase, they were treated with SP-MEL and the building components. For the cell viability measurements 10×, 30× and 100× dilutions from SP-MEL formulation as well as 2.5 mg/ml MEL suspension, 83.3 mg/ml D-trehalose dihydrate, 16.7 mg/ml SP solutions, corresponding to the concentration of components in SP-MEL formulation were prepared in cell culture medium.

2.8. Permeability study on the cell culture model

For the permeability experiments RPMI 2650 cells were cultured on inserts (Transwell, polycarbonate membrane, 3 µm pore size, 1.12 cm^2, Corning Costar Co., MA, USA) placed in

12-well plates in the presence of endothelial cells for 5 days (Figure 1). To prepare the co-culture model, endothelial cells were passaged (1×10^5 cells/cm^2) to the bottom side of tissue culture inserts coated with low growth factor containing Matrigel (BD Biosciences, NJ, USA) then the cells were kept in an incubator for 3 hours. After cell adhesion, cell culture inserts were placed in 12-well culture dishes containing 1.5 ml of endothelial culture medium, and RPMI 2650 nasal epithelial cells were pipetted (2×10^5 cells/cm^2) onto the upper surface of the membrane, which were coated with rat tail collagen previously. The establishment of the co-culture model is illustrated in Figure 1.

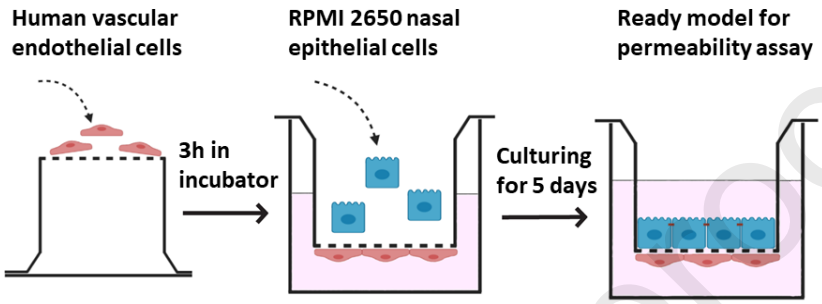

Figure 1. The assembly of the human nasal epithelial cell and vascular endothelial cell co-culture model.

Transepithelial electrical resistance (TEER) was measured to check the barrier integrity by an EVOM voltohmmeter (World Precision Instruments, USA) combined with STX-2 electrodes, and was expressed relative to the surface area of the monolayers as $\Omega \times cm^2$. TEER of cell-free inserts was subtracted from the measured data. After the cell layer reached steady TEER values, the cells were treated. For the permeability experiments the inserts were transferred to 12-well plates containing 1.5 ml Ringer-HEPES buffer in the acceptor compartments. In the donor compartments 0.5 ml buffer was pipetted containing MEL or the SP-MEL polymeric micelle formulation. In static *in vitro* models the unstirred water layer above the barrier forming cells slows molecular diffusion and affects the P_{app} of compounds (Youdim et al. 2003). To reduce the formation of this aqueous layer and increase the reproducibility of results a moderate shaking procedure is suggested for permeability assays (Youdim et al. 2003). In our experiments the plates were kept on a horizontal shaker (120 rpm; PSU-2T, Biosan, Riga, Latvia) during the assay which lasted for 60 min. Samples from both compartments were collected and the MEL concentration was measured by HPLC. To determine the tightness of the nasal epithelial co-culture model two passive permeability marker molecules were tested after the permeability experiment. In the donor compartments 0.5 ml buffer containing fluorescein isothiocyanate (FITC)-labeled dextran (FD10, 10 µg/ml; Mw: 10 kDa) and Evans blue labeled albumin (167.5 µg/ml Evans blue dye and 10 mg/ml bovine serum albumin; MW: 67.5 kDa) was added. The inserts were kept in 12-well plates on a horizontal shaker (120 rpm) for 30 min. The concentrations of the marker molecules in the samples from the compartments were determined by a fluorescence multiwell plate reader (Fluostar Optima, BMG Labtechnologies, Germany; FITC: excitation wavelength: 485 nm, emission wavelength: 520 nm; Evans-blue labeled albumin: excitation wavelength: 584 nm, emission wavelength: 680

nm). The apparent permeability coefficients (P_{app}) were calculated as described previously (Bocsik et al., 2019). Briefly, cleared volume was calculated from the concentration difference of the tracer in the acceptor compartment ($\Delta[C]_A$) after 30 min and in donor compartments at 0 hour ($[C]_D$), the volume of the acceptor compartment (V_A; 1.5 ml) and the surface area available for permeability (A; 1.1 cm^2) using this equation:

$$P_{app}\left(\frac{cm}{s}\right) = \frac{\Delta[C]_A x\, V_A}{A\, x\, [C]^D x \Delta t} \quad (1)$$

For the permeability measurement, 2.5 mg/ml MEL and 10× dilution of SP-MEL were prepared in Ringer-Hepes buffer and added to the donor compartments.

2.9. Immunohistochemistry

To evaluate morphological changes in RPMI 2650 cells caused by the MEL-loaded polymeric micelle formulation, immunostaining for junctional proteins zonula occludens protein-1 (ZO-1) and β-catenin was made. After the permeability experiments, cells on culture inserts were washed with phosphate buffer (PBS) and fixed with ice cold methanol-acetone (1:1) solution for 2 min then washed with PBS. The nonspecific binding sites were blocked with 3% bovine serum albumin in PBS. Primary antibodies rabbit anti-ZO-1 (AB_138452, 1:400; Life Technologies, USA) and rabbit anti-β-catenin (AB_476831, 1:400) were applied as overnight treatment at 4 °C. Incubation with secondary antibodies anti-rabbit IgG Cy3 conjugated (AB_258792, 1:400) lasted for 1 hour and Hoechst dye 33342 was used to stain cell nuclei. After mounting the samples (Fluoromount-G; Southern Biotech, USA) staining was visualized by Leica TCS SP5 confocal laser scanning microscope (Leica Microsystems GmbH, Germany).

2.10. *Ex vivo* semiquantitative permeability study across nasal mucosa

Ex vivo permeability tests were performed on human nasal mucosa (mucoperiosteum). The pieces of the nasal mucosa for primary study were collected during daily clinical routine nasal and sinus surgeries (septoplasty) under general or local anesthesia. The patients were all female between 40 and 50 years. The surgical field was infiltrated with 1 % w/v Lidocain-Tonogen local injection and the mucosa was lifted from its base with a raspotirum or Cottle elevator. Transport from the operating room to the laboratory is performed in physiological saline solution. All experiments were performed freshly after the removal of the tissue. The experiments have been carried out under approval of University of Szeged's institutional ethics committee (ETT-TUKEB: IV/3880-1/2021/EKU). The nasal mucosa was excised with surgical scalpel into uniform square segments with a diameter of 6 mm to provide appropriate are of the semiquantitative study and it would fit into the membrane inserts for the later described quantitative study.

5 µl of MEL suspension (2.5 mg/ml) and the SP-MEL formulation have been instilled on the epithelial surface of the nasal mucosa. After an incubation time of 1 h at 37 °C, the formulations were washed twice with physiological saline solution and the nasal mucosa was divided into 20 µm thick cross-sections into the incision point (Leica CM1950 cryostat (Leica Biosystems GmbH, Wetzlar, Germany), then inverted to the cross-sectional side and placed on aluminum foil-coated glass slides. *Ex vivo* Raman chemical mapping was performed to describe the

penetration pattern of the polymeric micelle formulation across the nasal mucosa using a ThermoFisher XRD Dispersive Raman instrument (ThermoFisher Scientific Inc., Waltham, MA, USA) equipped with a CCD camera and a diode laser operating at the wavelength of 780 nm. A 500 µm × 500 µm surface was analyzed with a step size of 50 µm. The exposure time was set at 4 s with an acquisition time of 4 s, for a total of 16 scans per spectrum in the spectral range of 3500 to 200 cm^{-1}. Cosmic-ray and fluorescence corrections have been performed. The Raman spectra were normalized to eliminate the intensity deviation between the measured areas (Sipos et al., 2020).

2.11. *Ex vivo* quantitative permeability study across nasal mucosa

To investigate *ex vivo* the transmucosal passive diffusion, a modified Side-Bi-Side® type horizontal diffusion apparatus was applied. The setting was previously developed by our research team and is validated to investigate nasal powders and liquids as well. For further information, Gieszinger et al. reported the apparatus with proper description (Gieszinger et al., 2021). The diffusion of MEL suspension (2.5 mg/ml) and SP-MEL formulation was tested across the excised human nasal mucosa. The nasal mucosa was mounted between the donor and the acceptor compartments with a diffusion surface area of 0.785 cm^2 completely covering the membrane insert hole with a diameter of 5 mm. The donor was prepared by mixing 1.0 ml of the formulations with 8.0 ml of SNES while the acceptor phase contained 9.0 ml of pH 7.4 PBS to simulate nasal conditions. The temperature of the chambers was controlled at 35 ± 0.5 °C using a heating circulator (ThermoHaake C 10-P5, Sigma-Aldrich Co., Ltd., Budapest, Hungary). The compartments were continuously stirred at 100 rpm using magnetic stirrers. 100 µl aliquots from the acceptor phase were taken at predetermined time points and immediately replaced with fresh medium. The concentration of MEL was determined by HPLC. The flux (J (µg/cm^2/h)) was calculated from the permeated drug quantity through the nasal mucosa (m_t), divided by the surface of the membrane insert (A) and the duration of the investigation (t) (Eq. 2). The permeability coefficient (K_p (cm/h)) was determined by dividing the flux (J) with the drug concentration in the donor phase (Cd (µg/cm^3)) (Sipos et al., 2021; Sipos et al., 2022).

$J = \frac{m_t}{A\,x\,t}$	(2)
$K_p = \frac{J}{C_d}$	(3)

2.12. *In vivo* animal studies

All the experiments involving animal subjects were carried out with the approval of the National Scientific Ethical Committee on Animal Experimentation (permission number: IV/1247/2017). The animals were treated in accordance with the European Communities Council Directives (2010/63/EU) and the Hungarian Act for the Protection of Animals in Research (Article 32 of Act XXVIII). A 60-µg dose of MEL from the 2.5 mg/ml SP-MEL formulation was administered into the right nostril of 160 – 180 g male Sprague Dawley rats (n = 24) via a pipette. At predetermined time points (5, 15, 30, 60, 120 and 240 min), the blood of the rats (under

isoflurane anesthesia) was collected into heparinized tubes via cardiac puncture. Then, the animals were sacrificed by decapitation and brain tissues were removed, rinsed in ice-cold PBS, weighed and stored at – 80 °C until assayed.

Plasma samples were centrifuged at 1500 × g for 10 min at 5 °C. To 100 µl of plasma sample, 10 µl of 0.1 % w/v aqueous formic acid and 330 µl acetonitrile containing 110 ng piroxicam (internal standard) were added and the mixture was spun for 60 s. The mixture was allowed to rest for 30 min at – 20 °C to support protein precipitation. The supernatant was obtained via the centrifugation of the mixture for 10 min at 10,000 × g at 4 °C. 20 µl of clear supernatant was diluted using 380 µl 0.1 % w/v aqueous formic acid and stirred for 30 s. 5 µl was injected into the LC-MS/MS system for analysis. The rat plasma calibration standards of MEL were prepared by moving the working standard solutions (in concentration range between 234 to 5000 ng/ml) into a pool of drug-free rat plasma. The sample preparation procedure described above was followed. The sample preparation procedure described above was followed.

Whole brain (1.6 to 2.0 g) of rats were homogenized in 1 % v/v aqueous acetic acid (1 g tissue/4 mL) using an UCD-500 ultrasonic cell disrupter (Biobase Biodustry, Shandong, China) in an ice bath for 2 min, interrupted by cooling. To 200 µL of brain homogenate, 10 µL of 0.1 % w/v aqueous formic acid and 630 µL ice cold acetonitrile containing 1.6 ng piroxicam (internal standard) and 40 µL 0.1 M perchloric acid were added. The mixture was vortex-mixed for 60 s and allowed to rest for 30 min – 20 °C. After centrifugation for 10 min at 10,000 × g at 4 °C, 100 µL supernatant was diluted with 100 µL of 0.1 % w/v aqueous formic acid, vortexed and 20 µL was analyzed by LC–MS/MS. Rat brain calibration standards of MEL were prepared by moving the working standard solutions (in concentration range between 2.35 to 50 ng/mL) into a pool of drug-free rat brain homogenate. The sample preparation procedure described above was followed.

2.13. LC-MS/MS analysis of *in vivo* studies

The quantitative analysis of MEL was performed by using a Waters Acquity I-Class UPLCTM system (Waters, Manchester, UK), connected to a Q Exactive™ Plus Orbitrap mass spectrometer (Thermo Fisher Scientific, San Jose, CA, USA) equipped with a heated ESI ion source (HESI). Gradient chromatographic separation was performed at room temperature on a Acquity BEH C18 column (50 mm × 2.1 mm, particle size 1,7 µm) protected by a C18 guard column (2 × 2 mm, Phenomenex, Torrance, CA, USA) by using 0.1% aqueous formic acid as Solvent A and acetonitrile with 0.1% formic acid as Solvent B. The gradient applied for the analysis can be seen in Table 1.

Table 1. Gradient applied for the analysis of MEL using LC-MS/MS analysis for the *in vivo* studies.

Time (min)	Eluent A (%)	Eluent B (%)	Flow rate (µl/min)
0	65	35	300
2	45	55	300

2.1	0	100	600
2.6	0	100	600
2.7	65	35	600
3.7	65	35	600
3.8	65	35	300
4.5	65	35	300

The mass spectrometer was used in a positive mode with the following parameters of the HESI source: spray voltage at 3.5 kV, capillary temperature at 256 °C, aux gas heater temperature at 406 °C, sheath gas flow rate at 47.5 l/h, aux gas flow rate at 11.25 l/h, sweep gas flow rate at 2.25 L/h, and S-lens radio frequency (RF) level at 50.0 (source auto-defaults). Parallel-reaction-monitoring (PRM) mode was used for quantifying by monitoring the following transitions: m/z 352 → 115 for MEL and m/z 332 → 95 for piroxicam. Due to the low concentrations of MEL in the biological samples, piroxicam was applied in order to achieve the analysis via standard addition and the transition degree matches with MEL as they are similar in structure. The normalized collision energies (NCEs) for specific quantification were optimized to maximize the sensitivity. The NCEs were 24 for MEL and 29 for piroxicam. A valve placed after the analytical column was programmed to switch the flow onto MS only when analytes of interest elute from the column (1.15–2.15 min) to prevent excessive contamination of the ion source and ion optics. Washing procedures of the autosampler before and after injecting samples were programmed in order to avoid the carry-over of analytes. Data acquisition and processing were carried out using Xcalibur and Quan Browser (version 4.5.474.0) software (Thermo Fisher Scientific, San Jose, CA, USA).

2.14. Pharmacokinetic studies

Pharmacokinetic parameters were analyzed via PK Solver 2.0 Software through non-compartmental analysis of the measured brain and plasma data. The area under the curve (AUC) of the time (min) – concentration curves of each animal were fitted with a linear trapezoidal method (Alshweiat et al., 2020). All reported data are means ± SD.

3. Results and discussion

3.1. *In vitro* mucoadhesion study

Based on the previous results mentioned earlier regarding the SP-MEL formulation, adequate nasal administration can be achieved due to its physicochemical properties. The adhesion to the nasal mucosa, expressed as mucoadhesion, plays a pivotal rule in the successful and efficient absorption of nanocarriers through the nasal route by increasing the residence time of intranasal administered formulations inhibiting the rapid elimination through mucociliary clearance. Mucoadhesive properties of polymeric micelle forming polymers can be characterized with good features. The surface residence time provided by the polymer depends on its ability to form physical and/or chemical secondary bonds (e.g., hydrogen bonds) between the outer shell and the nasal mucosa. SP itself in aqueous solution forms polymeric micelles where the shell's

surface is covered by hydroxyl groups originated from the PEG 6000 chain. This allows bond formation, therefore increased residence time (Ascentiis et al., 1995; Shojaei and Li, 1997). To test whether the adhesive force needed to separate the formulation from the simulated nasal membrane and the adhesive work referring to the whole mucoadhesion process are influenced by MEL loading, tensile test was applied (Sipos et al., 2021). Based on the results in Figure 2., no significant ($p > 0.05$, not significant) decrease can be experienced after drug loading. A slight decrease can be justified by the orientation of polymeric chains towards the hydrophilic molecule parts of MEL; however, a moderately high force and work can be claimed about the formulation itself. Another advantage of this result is that via this moderate mucoadhesion, rapid drug release is expected and tested *in vitro* before (Sipos et al., 2020), therefore not hindering the quick transport of the nanocarriers via either nose-to-blood or nose-to-brain transport. It is also clearly indicated that strong mucoadhesion cannot be claimed about the formulations compared to a commonly applied mucoadhesive agent in a typical concentration, which is a 0.5% w/v hyaluronic acid solution. Without mucin, negligible adhesion properties could be experienced which also indicates that the main forces occur between the formulation and the mucin itself. Thus, as the value of mucoadhesive force and work regarding the formulation and the co-polymer SP solution lies in between these values, a moderately high mucoadhesion can characterize the product.

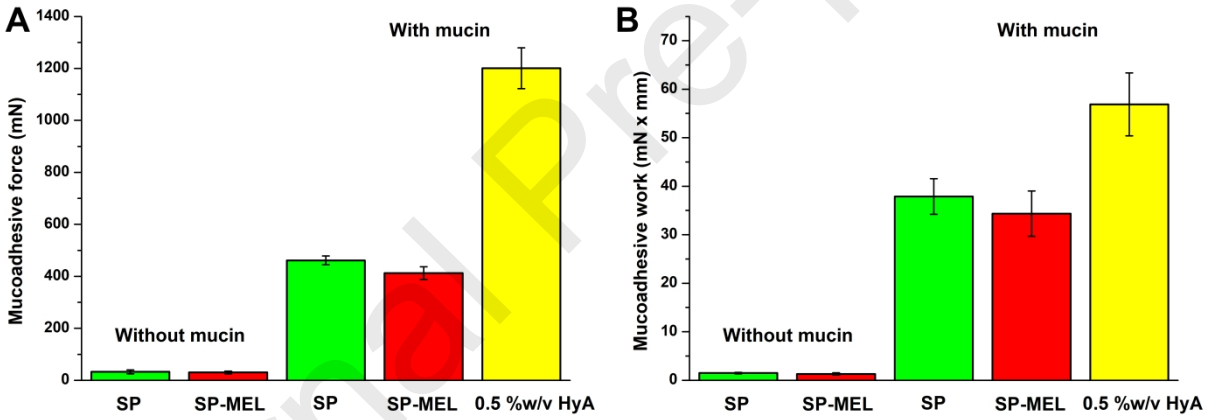

Figure 2. Mucoadhesive force (A) and mucoadhesive work (B) measured during the tensile test. The column diagram represents the average of 5 measurements with standard deviation. Statistical analysis: n.s. (not significant), $p > 0.05$. As positive control 0.5% w/v hyaluronic acid (HyA) solution was applied and as negative controls, mucinless experiments were carried out.

3.2. Cell viability assay

The potential toxicity of polymeric nanoparticles is the main problem concerning their use in medicine, however due to their specificity and efficacy, their utilization as advanced drug delivery systems in targeted drug delivery shows a growing demand (Patel et al., 2021). Therefore, to dispel the toxicity concerns in terms of the developed formulation, cell viability assay was conducted. Impedance measurement, as a sensitive method to detect alternation in cellular viability, did not show cell damage after the 1-hour treatment of the tested SP-MEL formulation or its own components (Figure 3). Different dilution series was investigated for each component representing the dilution process in the nasal cavity. The measured and calculated normalized cell index percentages remained in the adequate ratio compared to the

control group. As a reference compound to cause cell death, Triton X-100 detergent was applied which decreased cell impedance to baseline (Figure 3). No significant difference ($p > 0.05$) in the normalized cell index was obtained in case of neither MEL, SP, D-TRE nor SP-MEL in comparison to control group. These results contribute to the fact that SP-MEL can be safely administered through the nasal cavity as previous studies has also proved and also it reflects to the non-toxic behavior of SP as well on RPMI 2650 cell line. Similar results were obtained by Alopaeus et al. according to which even a 10 % w/w SP solution did not show cytotoxic effect on HT29-MTX cell lines (Alopaeus et al., 2019). Moreover, it has been revealed SP was biocompatible towards mucus-producing HT29-MTX cells, indicating no inhibition in mucin secretion, therefore, change in mucoadhesive properties.

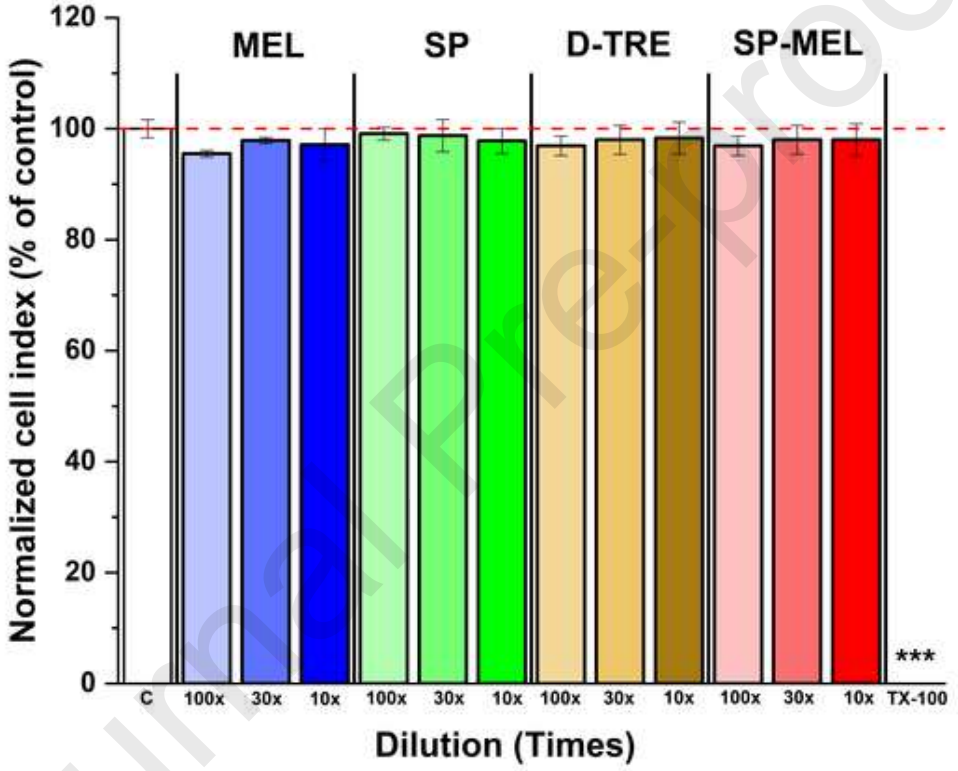

Figure 3. Cell viability of RPMI 2650 nasal epithelial cells after 1-hour treatment with meloxicam, the nanoformulations or their components measured by impedance. The values presented as a percentage of the control group. Values are presented as means ± SD, n = 6-12. Statistical analysis: ANOVA followed by Dunett's test. ***$p < 0.01$, compared to the control group. TX-100, Triton X-100 detergent.

3.3. MEL permeability across the culture model of the nasal mucosa barrier

The permeability of MEL was tested on the co-culture model composed of nasal epithelial and vascular endothelial cells. After 1-hour treatment, the SP-MEL formulation showed a 5-fold increase of MEL across this co-culture model (Figure 4.). The significantly higher (***, $p <$

0.001) apparent permeability values can be due to the fact of the permeation enhancer effect of SP across biological barriers along with the nano particle size.

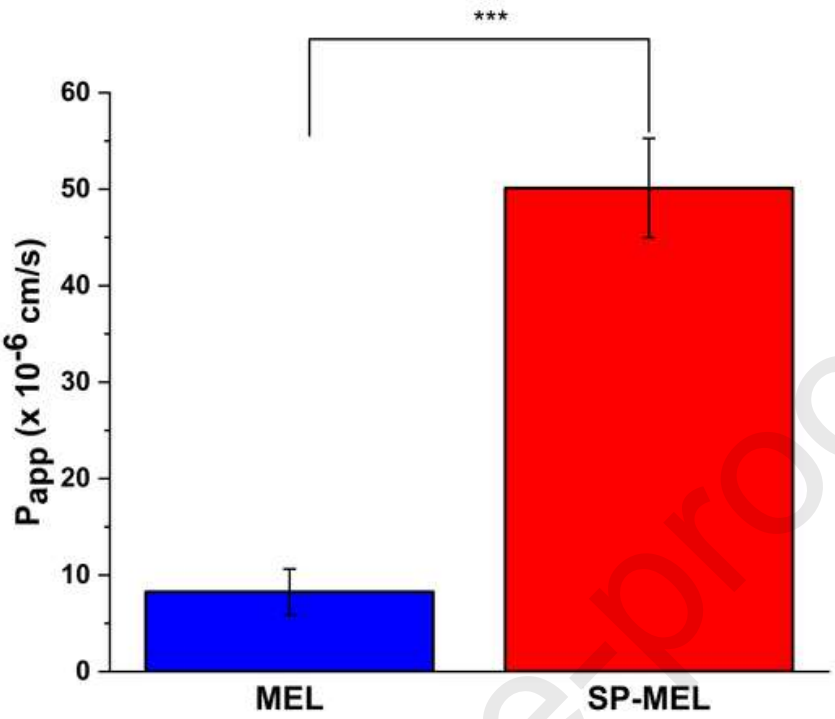

Figure 4. Apparent permeability of MEL (2.5 mg/ml in all samples) and MEL in SP-MEL nanoformulation across a co-culture model of human RPMI 2650 nasal epithelial cells and vascular endothelial cells (1-hour assay). Values are presented as means ± SD, n = 3. *** $p < 0.001$ significantly different from MEL control.

Our results about the permeability enhancement of SP across RPMI 2650 cell line is corroborated by the work of Pozzoli et al. where they found 2.5 times higher permeability of budesonide with SP as an excipient (Pozzoli et al., 2017). The higher degree of permeation in our case contributes to the fact that different dosage forms also affect the permeability. Whilst Pozzoli et al. formulated a freeze-dried nasal powder, our polymeric micelle formulation can utilize the benefits of a liquid state nasal formulation, whereas the API is in dissolved form allowing quicker and more efficient transport across the cells. Similarly other nanocarriers, such as human serum albumin nanoparticles were investigated on human RPMI 2650 cell line.

We found good TEER and low permeability values for paracellular markers indicating a good barrier property of the nasal mucosa co-culture model (Figure 5A) The TEER values remained at the level of the control group after 1-hour treatment with the SP-MEL formulation indicating that it does not damage the barrier function. MEL increased TEER and all three treatments decreased P_{app} values for the two hydrophilic paracellular marker molecules, dextran and albumin (Figure 5B). As previous studies also proved with other nanocarriers, this result suggests that MEL may have a beneficial effect on the nasal barrier either by itself or in separate formulations.

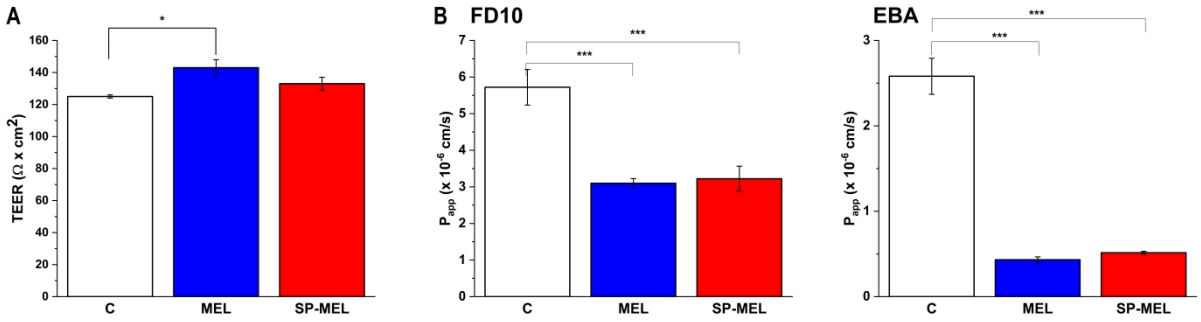

Figure 5. (A). Transepithelial electrical resistance (TEER) of the co-culture model after 1-hour treatment with MEL and SP-MEL (B) Values for paracellular permeability markers fluorescein isothiocyanate-labelled dextran (FD10) and Evans blue labelled albumin (EBA) after 1-hour treatment with MEL and SP-MEL. Values are presented as means ± SD, n = 3. C: control. * $p < 0.05$; *** $p < 0.001$ significantly different from control.

3.4. Immunhistochemistry

The change in the staining pattern of the junctional linker proteins ZO-1 and β-catenin was investigated on human RPMI 2650 nasal epithelial cells in the co-culture model to detect whether the SP-MEL formulation affects natural membrane integrity. The cells were typical cobblestone shaped with visible junctional proteins in a belt-like manner bordering the cells. No change in the staining pattern can be observed after the 1-hour treatment of the model with MEL and SP-MEL formulation compared to the control group which received only medium (Figure 6.). This microscopic imaging also contributes to the safe and non-toxic administration of polymeric micelle formulation. The results also exclude that classic surfactant-like permeation enhancement are achieved via SP as classic surfactants usually damage the barrier model unlike in our case.

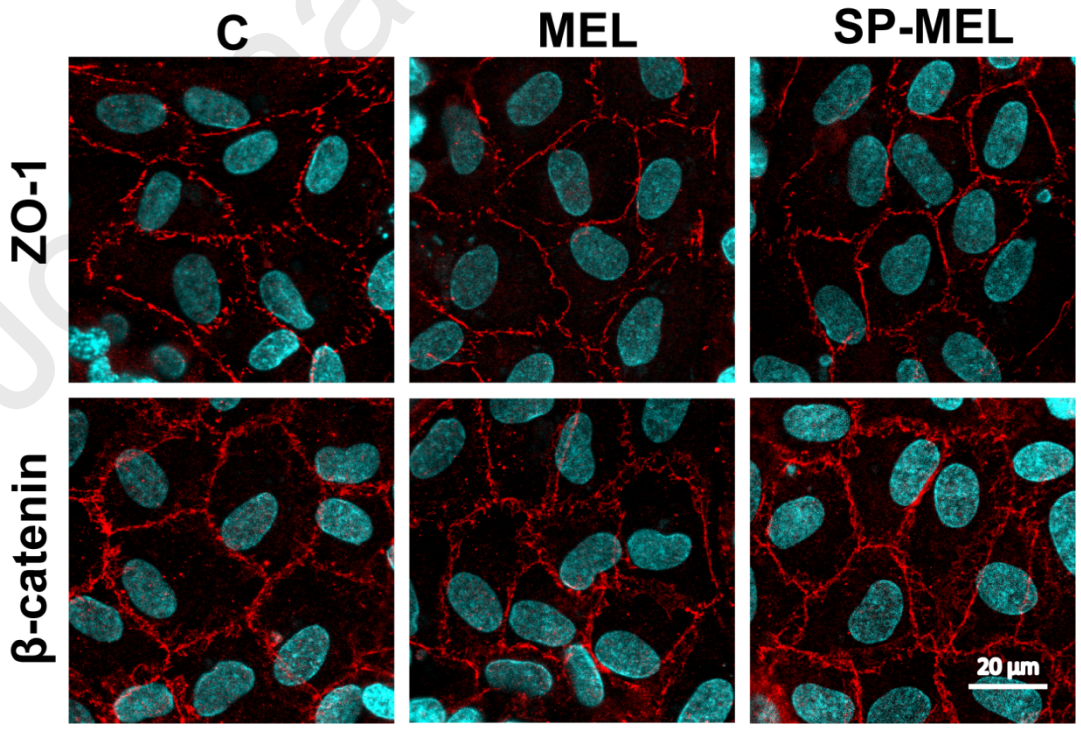

Figure 6. Immunostaining for junctional linker proteins ZO-1 and β-catenin on human RPMI 2650 nasal epithelial cell layers following a 1-hour treatment with MEL and SP-MEL. The control group (C) received only medium. Red: junctional proteins; blue: cell nuclei. Scale bar: 20 μm.

3.5. *Ex vivo* permeability measurements across nasal mucosa

Ex vivo permeability measurements across the nasal mucosa was carried out in order to investigate the permeation enhancement of MEL via SP compared to the reference MEL suspension. Semiquantitative investigation was performed via Raman spectroscopy after instillation upon the mucosal surface. The characteristic absorption peaks of MEL (at 1305 cm^{-1} (ν_{OH}), 1267 cm^{-1} (ν_{C-N-C}) and 1164 cm−1 (ν_{C-S}) were fitted on the surface map acquired via Raman chemical mapping (Figure 7.)

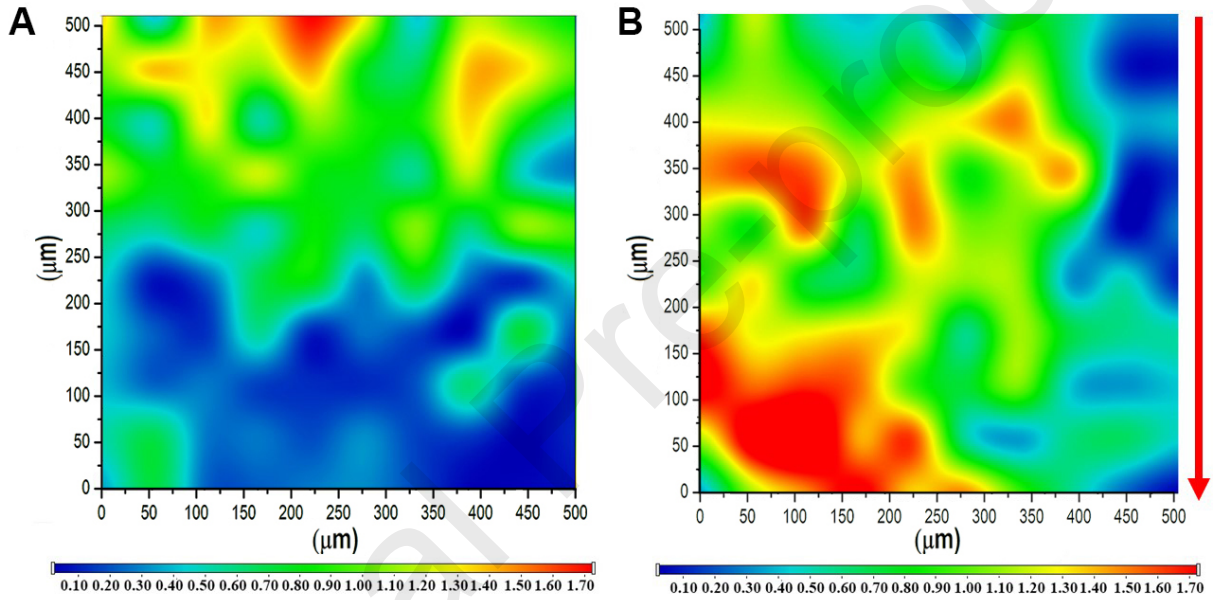

Figure 7. *Ex vivo* semiquantitative permeability measurement of MEL (A) and SP-MEL (B) across human nasal mucosa. The red arrow indicates the direction of transport across the incised tissue region. The Raman spectra were normalized.

Based on Figure 7, a deeper tissue penetration can be achieved via administering the SP-containing MEL formulation. SP can penetrate into deeper tissue regions compared to a regular, excipient-free formulation. This penetration is not cell damaging as the nasal cytotoxicity and immunohistochemistry investigations proved. This mechanism however is still similar to classic surfactant-based permeation enhancement (e.g., in the case of Tween 20), where the main leading force is that the API would transfer to the highly vascularized tissue regions.

The investigation was performed in a modified Side-bi-Side® type horizontal diffusion cell apparatus, where the cut tissue was mounted between the donor and acceptor compartments. The flux and permeability were evaluated after the quantification of aliquots in the acceptor compartment at predetermined time periods (Figure 8).

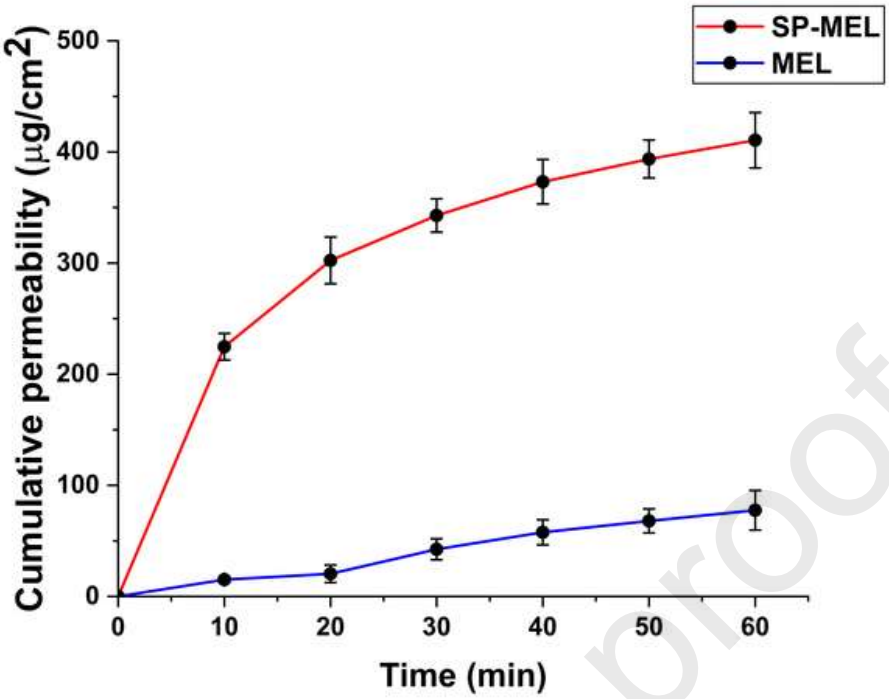

Figure 8. *Ex vivo* quantitative permeability study performed in a modified Side-bi-Side® type horizontal diffusion cell. The cumulative permeability values depicted at predetermined sampling time points in case of SP-MEL polymeric micelle formulation and the reference MEL suspension. All measurements were carried out in triplicate and data are presented as means ± SD (n=3).

The higher cumulative permeability values refer to the amount of permeated MEL across the tissue. The solubility enhancement induced increased permeability is caused by the SP micelle-forming polymer. As the *in vitro* drug release study showed in our previous study, a burst-like drug release can be experienced which corroborates that no lag time is needed to achieve the increased concentrations. The calculated flux is 410.54 μg/cm^2 at the final time point and the permeability coefficient is 0.493 cm/h which values are significantly higher than in case of MEL suspension: 77.491 μg/cm^2 and 0.068 cm/h (** $p < 0.01$ in both cases).

3.6. *In vivo* animal studies

To determine the promotion tendency of SP regarding MEL administration to the central nervous system, *in vivo* measurements were performed. The experiment lasted 4 hours, where at predetermined time points aliquots were withdrawn from the plasma and in the brain after the under-anaesthesia sacrifice of animals (Figure 9).

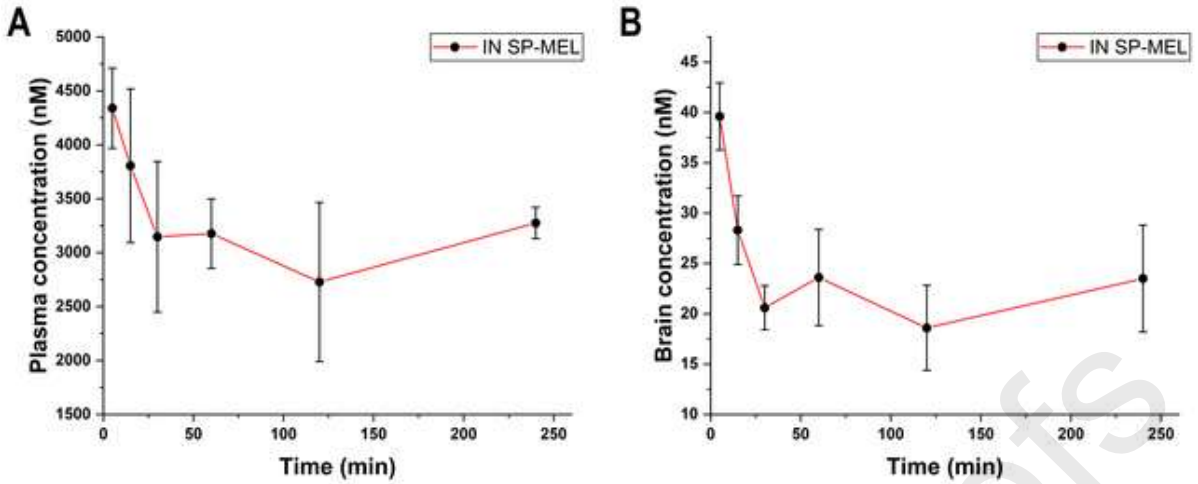

Figure 9. *In vivo* plasma (A) and brain (B) concentration of MEL after the intranasal (IN) treatment with the SP-MEL polymeric micelle nanoformulation. Results are expressed as average ± SD (n=4).

Our results can be compared by our research group's intranasal *in vivo* measurements, where physical particle size reduction techniques were applied on MEL (Bartos et al., 2018). Spray-drying was applied as reduction method, and the achieved MEL concentration in the brain was less than 1 nM. Compared to our results, approx. 35 to 40-times higher concentrations were achieved. The higher AUC values (approx. 35 nmol/ml x min in case of spray dryed formulations vs. approx. 5000 nmol/ml × min in case of SP-MEL formulation) also contributes to the fact that higher effective MEL transport was achieved to the central nervous system (Table 2). This shows the superiority of encapsulation into nanocarriers, as not only the decreased size resulted increased surface area is of paramount importance, but the need for permeability enhancers is there. Based on these and the *ex vivo* permeation results, SP formed micelles can penetrate into the deeper nasal regions where the uptake via the richly vascularized nasal mucosa region. As the olfactory nerves are innerved around this region, high chance of direct nose-to-brain transport can also be assumed. The brain curves have a maximum at 5 minutes which support this theorem, and the other maximum can be found at 60 minutes which can be identified as the typical nose-to-blood mediated brain transport time. The curves are not drastically decreasing after 2 hours, leaving the opportunity that a long-lasting and constant permeation to the CNS can occur. The supporting pharmacokinetic parameters can be found in Table 2.

Table 2. Calculated pharmacokinetic parameters regarding the intranasally administered SP-MEL formulation. All data are presents as means ± SD (n=4). Abbreviations: K_e – elimination rate constant; $t_{1/2}$ – half-time; AUC_{0-t} – area under curve value between 0 and the measurement time (t); $AUC_{0-\infty}$ -area under curve value between 0 and infinity; Cl – Clearance; MRT – mean residence time.

Pharmacokinetic parameter	Plasma	Brain
K_e (min^{-1})	$0.00091 \pm 2.2 \cdot 10^{-4}$	$0.00132 \pm 3.6 \cdot 10^{-5}$
$t_{1/2}$ (h)	804.143 ± 22.362	525.174 ± 14.378
AUC_{0-t} (µmol/ml x min)	811.228 ± 12.281	5.263 ± 0.051
$AUC_{0-\infty}$ (µmol/ml x min)	5115.035 ± 124.78	22.991 ± 0.674
Cl (µg/kg)/(nmol/ml)/min	$7.6 \cdot 10^{-5} \pm 1.6 \cdot 10^{-5}$	$0.0163 \pm 4.8 \cdot 10^{-4}$
MRT (min)	1197.25 ± 315.44	796.337 ± 23.17

Based on the pharmacokinetic investigations and calculations, the following can be stated. The AUC values regarding the brain concentration of MEL after intranasal administration of SP-MEL are significantly higher compared to the previously measured particle size-reduced MEL formulation. The clearance of SP-MEL and the high value of the MRT value indicates that a slow elimination process could be experienced in case of the nanocarrier. Besides the initial burst, based on these parameters a long-lasting effect can also be observed due to the previously mentioned fact that polymeric micelles could provide a higher circulation stability. Since the plasma concentration after IN administration followed the natural elimination curve with the high presence of MEL in the brain, the nose-to-brain pathway is more likely in the early stages after administration, however the long elimination can contribute to later penetration across the BBB as well. This is supported by the results of *in vitro* cell line and *ex vivo* nasal mucosa permeation studies where intensive, rapid, burst-like permeation could be found which is a potential sign that the immensely innervated nasal mucosa also takes up the active substance towards the neural pathway. Since the polymeric micelle formulation had a negative zeta potential value, carrier-intact paracellular or transcytosis-type permeation could also be a possibility in our case.

4. Conclusion

In conclusion, we successfully proved our hypothesis by the detailed *in vitro* to *in vivo* nasal applicability studies. Based on our previous experience and results, the *in vitro* characterization offered a promising solution for the SP-MEL formulation to be further investigated. Alongside the proper physicochemical parameters, the general mucoadhesive tendency of SP is not significantly lowered after the loading of MEL in the system. It is not high enough to offer the same residence time as a gelling system, however it contributes to a proper adhesion to the nasal mucosa where, based on our cell line studies, a rapid and highly efficient MEL transport can be achieved. This enhanced permeation takes place without the damaging properties of commonly applied surfactant molecules and SP proved to be safe to administer. *Ex vivo* studies also confirmed the high tissue permeation followed by the *in vivo* pharmacokinetic characterization of our formulation. High brain concentrations were achieved with the SP-MEL formulation compared to prior results achieved via physical particle size reduction techniques. Our results offer the utilization of this nanocarrier system as a tool to efficiently transport non-steroidal anti-inflammatory agents as possible remedies to inflammation-based and/or inflammation-associated neural diseases.

Acknowledgements

This work was supported by Project no. TKP2021-EGA-32 implemented with the support provided by the Ministry of Innovation and Technology of Hungary from the National Research, Development and Innovation Fund, financed under the TKP2021-EGA funding scheme. S.V. was supported by the Premium Postdoctoral Research Program (Premium-2019-469) of the Hungarian Academy of Sciences and the OTKA Young Researcher Excellence Program (OTKA-FK 143233) by National Research, Development and Innovation Office of Hungary.

Conflicts of interest

The authors report no conflicts of interest. The authors alone are responsible for the content and writing of this article.

References

M. Agrawal, S. Saraf, S. Saraf, S.G. Antimisiaris, M.B. Chougule, S.A. Shoyele, A. Alexander, Nose-to-brain drug delivery: An update on clinical challenges and progress towards approval of anti-Alzheimer drugs, J. Control. Release. 281 (2018) 139–177. https://doi.org/10.1016/j.jconrel.2018.05.011.

J.F. Alopaeus, E. Hagesæther, I. Tho, Micellisation mechanism and behaviour of soluplus®–furosemide micelles: Preformulation studies of an oral nanocarrier-based system, Pharmaceuticals. 12 (2019) 1–23. https://doi.org/10.3390/ph12010015.

A. Alshweiat, Ii.I. Csóka, F. Tömösi, T. Janáky, A. Kovács, R. Gáspár, A. Sztojkov-Ivanov, E. Ducza, Á. Márki, P. Szabó-Révész, R. Ambrus, Nasal delivery of nanosuspension-based mucoadhesive formulation with improved bioavailability of loratadine: Preparation, characterization, and in vivo evaluation, Int. J. Pharm. 579 (2020) 119166. https://doi.org/10.1016/j.ijpharm.2020.119166.

C. Bartos, R. Ambrus, A. Kovács, R. Gáspár, A. Sztojkov-Ivanov, Á. Márki, T. Janáky, F. Tömösi, G. Kecskeméti, P. Szabó-Révész, Investigation of absorption routes of meloxicam and its salt form from intranasal delivery systems, Molecules. 23 (2018) 1–13. https://doi.org/10.3390/molecules23040784.

A. Bocsik, I. Gróf, L. Kiss, F. Ötvös, O. Zsíros, L. Daruka, L. Fülöp, M. Vastag, Á. Kittel, N. Imre, T.A. Martinek, C. Pál, P. Szabó-Révész, M.A. Deli, Dual action of the PN159/KLAL/MAP peptide: Increase of drug penetration across caco-2 intestinal barrier model by modulation of tight junctions and plasma membrane permeability, Pharmaceutics. 11 (2019). https://doi.org/10.3390/pharmaceutics11020073.

M. Budai-Szűcs, E.L. Kiss, B. Á. Szilágyi, A. Szilágyi, B. Gyarmati, S. Berkó, A. Kovács, G. Horvát, Z. Aigner, J. Soós, E. Csányi, Mucoadhesive cyclodextrin-modified thiolated poly(aspartic acid) as a potential ophthalmic drug delivery system, Polymers (Basel). 10 (2018). https://doi.org/10.3390/polym10020199.

M. Calvo-Rodríguez, L. Núñez, C. Villalobos, Non-steroidal anti-inflammatory drugs (NSAIDs) and neuroprotection in the elderly: A view from the mitochondria, Neural Regen. Res. 10 (2015) 1371–1372. https://doi.org/10.4103/1673-5374.165219.

J. Castile, Y.H. Cheng, B. Simmons, M. Perelman, A. Smith, P. Watts, Development of in vitro models to demonstrate the ability of PecSys®, an in situ nasal gelling technology, to reduce nasal run-off and drip, Drug Dev. Ind. Pharm. 39 (2013) 816–824. https://doi.org/10.3109/03639045.2012.707210.

R. Cecchelli, S. Aday, E. Sevin, C. Almeida, M. Culot, L. Dehouck, C. Coisne, B. Engelhardt, M.P. Dehouck, L. Ferreira, A stable and reproducible human blood-brain barrier model derived from hematopoietic stem cells, PLoS One. 9 (2014). https://doi.org/10.1371/journal.pone.0099733.

S.H. Choi, S. Aid, L. Caracciolo, S. Sakura Minami, T. Niikura, Y. Matsuoka, R.S. Turner, M.P. Mattson, F. Bosetti, Cyclooxygenase-1 inhibition reduces amyloid pathology and improves memory deficits in a mouse model of Alzheimer's disease, J. Neurochem. 124 (2013) 59–68. https://doi.org/10.1111/jnc.12059.

A. De Ascentiis, J.L. deGrazia, C.N. Bowman, P. Colombo, N.A. Peppas, Mucoadhesion of poly(2-hydroxyethyl methacrylate) is improved when linear poly(ethylene oxide) chains are added to the polymer network, J. Control. Release. 33 (1995) 197–201. https://doi.org/10.1016/0168-3659(94)00087-B.

M. Ghezzi, S. Pescina, C. Padula, P. Santi, E. Del Favero, L. Cantù, S. Nicoli, Polymeric micelles in drug delivery: An insight of the techniques for their characterization and assessment in biorelevant conditions, J. Control. Release. 332 (2021) 312–336. https://doi.org/10.1016/j.jconrel.2021.02.031.

P. Gieszinger, T. Kiss, P. Szabó-Révész, R. Ambrus. The development of an in vitro horizontal diffusion cell to investigate nasal powder penetration inline. Pharmaceutics. 13(6) (2021) 809. https://doi.org/10.3390/pharmaceutics13060809

M. Goldsmith, L. Abramovitz, D. Peer, Precision nanomedicine in neurodegenerative diseases, ACS Nano. 8 (2014) 1958–1965. https://doi.org/10.1021/nn501292z.

M.T. Heneka, M.J. Carson, J. El Khoury, G.E. Landreth, F. Brosseron, D.L. Feinstein, A.H. Jacobs, T. Wyss-Coray, J. Vitorica, R.M. Ransohoff, K. Herrup, S.A. Frautschy, B. Finsen, G.C. Brown, A. Verkhratsky, K. Yamanaka, J. Koistinaho, E. Latz, A. Halle, G.C. Petzold, T. Town, D. Morgan, M.L. Shinohara, V.H. Perry, C. Holmes, N.G. Bazan, D.J. Brooks, S. Hunot, B. Joseph, N. Deigendesch, O. Garaschuk, E. Boddeke, C.A. Dinarello, J.C. Breitner, G.M. Cole, D.T. Golenbock, M.P. Kummer, Neuroinflammation in Alzheimer's disease, Lancet Neurol. 14 (2015) 388–405. https://doi.org/10.1016/S1474-4422(15)70016-5.

S.S. Hong, K.T. Oh, H.G. Choi, S.J. Lim, Liposomal formulations for nose-to-brain delivery: Recent advances and future perspectives, Pharmaceutics. 11 (2019) 1–18. https://doi.org/10.3390/pharmaceutics11100540.

G. Horvát, B. Gyarmati, S. Berkó, P. Szabó-Révész, B.Á. Szilágyi, A. Szilágyi, J. Soós, G. Sandri, M.C. Bonferoni, S. Rossi, F. Ferrari, C. Caramella, E. Csányi, M. Budai-Szűcs, Thiolated poly(aspartic acid) as potential in situ gelling, ocular mucoadhesive drug delivery system, Eur. J. Pharm. Sci. 67 (2015) 1–11. https://doi.org/10.1016/j.ejps.2014.10.013.

G. Katona, G.T. Balogh, G. Dargó, R. Gáspár, Á. Márki, E. Ducza, A. Sztojkov-Ivanov, F. Tömösi, G. Kecskeméti, T. Janáky, T. Kiss, R. Ambrus, E. Pallagi, P. Szabó-Révész, I. Csóka, Development of meloxicam-human serum albumin nanoparticles for nose-to-brain delivery via application of a quality by design approach, Pharmaceutics. 12 (2020). https://doi.org/10.3390/pharmaceutics12020097.

G. Katona, B. Sipos, R. Ambrus, I. Csóka, P. Szabó-Révész, Characterizing the Drug-Release Enhancement Effect of Surfactants on Megestrol-Acetate-Loaded Granules, Pharmaceuticals. 15 (2022). https://doi.org/10.3390/ph15020113.

A.R. Khan, M. Liu, M.W. Khan, G. Zhai, Progress in brain targeting drug delivery system by nasal route, J. Control. Release. 268 (2017) 364–389. https://doi.org/10.1016/j.jconrel.2017.09.001.

L. Kürti, S. Veszelka, A. Bocsik, B. Ózsvári, L.G. Puskás, Á. Kittel, P. Szabó-Révész, M.A. Deli, Retinoic acid and hydrocortisone strengthen the barrier function of human RPMI 2650 cells, a model for nasal epithelial permeability, Cytotechnology. 65 (2013) 395–406. https://doi.org/10.1007/s10616-012-9493-7.

Y. Li, M. Li, T. Gong, Z. Zhang, X. Sun, Antigen-loaded polymeric hybrid micelles elicit strong mucosal and systemic immune responses after intranasal administration, J. Control. Release. 262 (2017) 151–158. https://doi.org/10.1016/j.jconrel.2017.07.034.

P.L. McGeer, E.G. McGeer, NSAIDs and Alzheimer disease: Epidemiological, animal model and clinical studies, Neurobiol. Aging. 28 (2007) 639–647. https://doi.org/10.1016/j.neurobiolaging.2006.03.013.

S.C. Owen, D.P.Y. Chan, M.S. Shoichet, Polymeric micelle stability, Nano Today. 7 (2012) 53–65. https://doi.org/10.1016/j.nantod.2012.01.002.

C.V. Pardeshi, V.S. Belgamwar, Direct nose to brain drug delivery via integrated nerve pathways bypassing the blood-brain barrier: An excellent platform for brain targeting, Expert Opin. Drug Deliv. 10 (2013) 957–972. https://doi.org/10.1517/17425247.2013.790887.

Patel, P., Vyas, N., & Raval, M. (2021). Safety and Toxicity issues of Polymeric Nanoparticles: A Serious Concern. Nanotechnology in Medicine: Toxicity and Safety, 156–173.

D.C.S. Pedroso, A. Tellechea, L. Moura, I. Fidalgo-Carvalho, J. Duarte, E. Carvalho, L. Ferreira, Improved survival, vascular differentiation and wound healing potential of stem cells co-cultured with endothelial cells, PLoS One. 6 (2011) 1–12. https://doi.org/10.1371/journal.pone.0016114.

I. Pepić, J. Lovrić, J. Filipović-Grčić, How do polymeric micelles cross epithelial barriers?, Eur. J. Pharm. Sci. 50 (2013) 42–55. https://doi.org/10.1016/j.ejps.2013.04.012.

M. Pozzoli, D. Traini, P.M. Young, M.B. Sukkar, F. Sonvico, Development of a Soluplus budesonide freeze-dried powder for nasal drug delivery, Drug Dev. Ind. Pharm. 43 (2017) 1510–1518. https://doi.org/10.1080/03639045.2017.1321659.

F. Sabir, G. Katona, R. Ismail, B. Sipos, R. Ambrus, I. Csóka, Development and characterization of N-propyl gallate encapsulated solid lipid nanoparticles-loaded hydrogel for intranasal delivery, Pharmaceuticals. 14 (2021). https://doi.org/10.3390/PH14070696.

Sanz-Blasco, S., Calvo-Rodriguez, M., Caballero, E., Garcia-Durillo, M., Nunez, L., Villalobos, C. (2018). Is it all said for NSAIDs in Alzheimer's disease? Role of mitochondrial calcium uptake. Current Alzheimer Research, 15(6), 504– 510.

C. Saraiva, C. Praça, R. Ferreira, T. Santos, L. Ferreira, L. Bernardino, Nanoparticle-mediated brain drug delivery: Overcoming blood-brain barrier to treat neurodegenerative diseases, J. Control. Release. 235 (2016) 34–47. https://doi.org/10.1016/j.jconrel.2016.05.044.

T. Shabab, R. Khanabdali, S.Z. Moghadamtousi, H.A. Kadir, G. Mohan, Neuroinflammation pathways: a general review, Int. J. Neurosci. 127 (2017) 624–633. https://doi.org/10.1080/00207454.2016.1212854.

V. Sharma, Neuroinflammation in Alzheimer's disease and involvement of interleukin-1: a mechanistic view, Int. J. Pharm. Sci. Drug Res. 3 (2011) 287–291.

A.H. Shojaei, X. Li, Mechanisms of buccal mucoadhesion of novel copolymers of acrylic acid and polyethylene glycol monomethylether monomethacrylate, J. Control. Release. 47 (1997) 151–161. https://doi.org/10.1016/S0168-3659(96)01626-4.

B. Sipos, I. Csóka, R. Ambrus, Z. Schelz, I. Zupkó, G.T. Balogh, G. Katona, Spray-dried indomethacin-loaded polymeric micelles for the improvement of intestinal drug release and permeability, Eur. J. Pharm. Sci. 174 (2022). https://doi.org/10.1016/j.ejps.2022.106200.

B. Sipos, I. Csóka, M. Budai-Szűcs, G. Kozma, D. Berkesi, Z. Kónya, G.T. Balogh, G. Katona, Development of dexamethasone-loaded mixed polymeric micelles for nasal delivery, Eur. J. Pharm. Sci. 166 (2021). https://doi.org/10.1016/j.ejps.2021.105960.

B. Sipos, P. Szabó-Révész, I. Csóka, E. Pallagi, D.G. Dobó, P. Bélteky, Z. Kónya, Á. Deák, L. Janovák, G. Katona, Quality by design based formulation study of meloxicam-loaded polymeric micelles for intranasal administration, Pharmaceutics. 12 (2020) 1–29. https://doi.org/10.3390/pharmaceutics12080697.

P. Sun, Y. Xiao, Q. Di, W. Ma, X. Ma, Q. Wang, W. Chen, Transferrin receptor-targeted peg-pla polymeric micelles for chemotherapy against glioblastoma multiforme, Int. J. Nanomedicine. 15 (2020) 6673–6688. https://doi.org/10.2147/IJN.S257459.

P. Szabó-Révész, Modifying the physicochemical properties of NSAIDs for nasal and pulmonary administration, Drug Discov. Today Technol. 27 (2018) 87–93. https://doi.org/10.1016/j.ddtec.2018.03.002.

N. Thotakura, P. Parashar, K. Raza, Assessing the pharmacokinetics and toxicology of polymeric micelle conjugated therapeutics, Expert Opin. Drug Metab. Toxicol. 17 (2021) 323–332. https://doi.org/10.1080/17425255.2021.1862085.

Z.N. Warnken, H.D.C. Smyth, A.B. Watts, S. Weitman, J.G. Kuhn, R.O. Williams, Formulation and device design to increase nose to brain drug delivery, J. Drug Deliv. Sci. Technol. 35 (2016) 213–222. https://doi.org/10.1016/j.jddst.2016.05.003.

M. Watanabe, K. Kawano, M. Yokoyama, P. Opanasopit, T. Okano, Y. Maitani, Preparation of camptothecin-loaded polymeric micelles and evaluation of their incorporation and circulation stability, Int. J. Pharm. 308 (2006) 183–189. https://doi.org/10.1016/j.ijpharm.2005.10.030.

S. Wohlfart, S. Gelperina, J. Kreuter, Transport of drugs across the blood-brain barrier by nanoparticles, J. Control. Release. 161 (2012) 264–273. https://doi.org/10.1016/j.jconrel.2011.08.017.

K.H. Wong, M.K. Riaz, Y. Xie, X. Zhang, Q. Liu, H. Chen, Z. Bian, X. Chen, A. Lu, Z. Yang, Review of current strategies for delivering Alzheimer's disease drugs across the blood-brain barrier, Int. J. Mol. Sci. 20 (2019). https://doi.org/10.3390/ijms20020381.

K.A. Youdim, A. Avdeef, N.J. Abbott, In vitro trans-monolayer permeability calculations: often forgotten assumptions. Drug Discov Today (2003) 8(21):997–1003. https://doi.org/10.1016/s1359- 6446(03)02873-3

L.Y. Zakharova, T.N. Pashirova, S. Doktorovova, A.R. Fernandes, E. Sanchez-Lopez, A.M. Silva, S.B. Souto, E.B. Souto, Cationic surfactants: Self-assembly, structure-activity correlation and their biological applications, 2019. https://doi.org/10.3390/ijms20225534.

O. Zanetti, P. Pasqualetti, C. Bonomini, G.D. Forno, L. Paulon, E. Sinforiani, C. Marra, P.M. Rossini, A randomized controlled study on effects of ibuprofen on cognitive progression of Alzheimer's disease* Aging Clinical and Experimental Research, Aging Clin Exp Res. 21 (2009) 102–110.

CRediT author statement

All authors have read and agreed to the published version of the manuscript.

Bence Sipos: conceptualization, methodology, software, formal analysis, investigation, data curation, writing -original draft preparation, visualization, project administration

Zsolt Bella: investigation, resources, writing – review and editing

Ilona Grósf: investigation, data curation, software, writing – original draft preparation

Szilvia Veszelka: investigation, data curation, writing – original draft preparation

Mária A. Deli: data curation, resources, formal analysis, writing – review and editing

Kálmán F. Szűcs: investigation, data curation, writing – review and editing

Anita Sztojkov-Ivanov: investigation, data curation, software, writing – review and editing

Eszter Ducza: investigation, data curation, writing – review and editing

Róbert Gáspár: investigation, resources, formal analysis, writing – review and editing

Gábor Kecskeméti: investigation, data curation, writing – review and editing

Tamás Janáky: investigation, resources, formal analysis, writing – review and editing

Balázs Volk: resources, formal analysis, writing – review and editing

Mária Budai-Szűcs: software, investigation, writing – original draft preparation

Rita Ambrus: conceptualization, validation, resources, writing – review and editing, project administration

Piroska Szabó-Révész: validation, resources, writing – review and editing

Ildikó Csóka: conceptualization, methodology, validation, formal analysis, resources, writing – review and editing, supervision, project administration, funding acquisition

Gábor Katona: conceptualization, methodology, validation, formal analysis, resources, writing – review and editing, supervision, project administration

Declaration of interests

☒ The authors declare that they have no known competing financial interests or personal relationships that could have appeared to influence the work reported in this paper.

☐ The authors declare the following financial interests/personal relationships which may be considered as potential competing interests:

Soluplus® promotes efficient transport of meloxicam to the central nervous system via nasal administration

Highlights

- Meloxicam-loaded micelles provided efficient cellular permeability
- The micelle formulation is applicable for the nasal administration
- Meloxicam-loaded nasal micelles achieved efficient concentration in the brain